AIAA JOURNAL
Vol. 30, No. 11, November 1992

Prediction of Interlaminar Stresses in Laminated Plates Using Global Orthogonal Interpolation Polynomials

Chansup Byun* and Rakesh K. Kapania†
Virginia Polytechnic Institute and State University, Blacksburg, Virginia 24061

A postprocessor for displacement-based finite element solutions of laminated plates under transverse loads is developed to obtain the resulting interlaminar stresses. The postprocessor can be used for the finite element solution that has been obtained using either the classical lamination plate theory or the first-order shear deformation theory. The equilibrium equations of elasticity are integrated directly to obtain interlaminar stresses. These equations include the influence of the products of in-plane stresses and out-of-plane rotations and thus can be used to obtain interlaminar stresses for geometrically nonlinear problems. To obtain accurately the derivatives of in-plane stresses, the finite element nodal displacement data are first interpolated using polynomials with global support (i.e., the interpolating polynomials are defined over the whole domain). Two types of polynomials, Chebyshev and a class of orthogonal polynomials that can be generated for a given location of known data points, are used. A least-squares technique is used to find the undetermined coefficients in the global approximation. For evaluation purposes, the results for interlaminar stresses for a set of examples obtained from the present code are compared with those obtained from exact three-dimensional theory of elasticity. A good agreement is shown. Furthermore, to the best of our knowledge, the present paper is the first to present the results for interlaminar normal stress in a two-layered antisymmetric angle-ply square plate without using the three-dimensional elasticity solution. It is observed that the shape of through-the-thickness distribution of interlaminar normal stress depends on the side-to-thickness ratio and that the maximum interlaminar normal stress increases rapidly as the side-to-thickness ratio increases.

Nomenclature

a,b = lengths of laminates in x and y directions, respectively
a_i,b_j = weighting functions in x and y directions, respectively
C_{ij} = coefficients of displacement approximations
h = total thickness of laminates
M^k = kth laminar moment resultants
N^k = kth laminar stress resultants
P_r = polynomial of degree r
p = interlaminar normal stress
Q^k = kth laminar shear resultants
S = side-to-thickness ratio
s,t = interlaminar shear stresses
w = out-of-plane displacement
ϵ = strains
κ = curvatures
σ = normal stresses
τ = shear stresses

Introduction

THE response of laminated structures to impact loads has been a problem of considerable interest and concern in recent years since laminated structures are vulnerable to the impact of a foreign object. When a laminated plate is struck by a hard object, flexural waves are produced, which may result in damages such as flexural failures on the outer layers, internal damage (delamination and intraply damage), and visible contact damage on the impacted surface. Because of the presence of weak links between various laminas, delamination can be initiated by interlaminar stresses and eventually may result in the ultimate failure of the laminate. Consequently, accurate determination of interlaminar stresses is a topic of interest. These interlaminar stresses can be computed directly using the constitutive equations when exact analytical solutions for the equilibrium equations of three-dimensional elasticity are available. Only a few exact elasticity solutions of interlaminar stresses for laminates subject to transverse loads are available (see, for example, Pagano[1,2] and Pagano and Hatfield[3]). For more general cases, however, analytical solutions to the three-dimensional elasticity equations are not available.

For arbitrarily laminated plates, approximate techniques based on the finite element method are often used to find the required response quantities, namely, displacements and stresses (including interlaminar stresses). One way of determining the interlaminar stresses is to use the constitutive equations directly if shear strains are available from the finite element program that has been derived using any of the existing shear deformation theories. The alternative is to integrate equilibrium equations of three-dimensional elasticity in the absence of body forces with respect to the thickness coordinate. The latter approach is more general in the sense that it can be adaptable to any displacement-based finite element program. Reddy[4] has shown that the latter approach could calculate interlaminar shear stresses more accurately.

Many researchers have obtained the interlaminar shear stresses by directly integrating the equilibrium equations of elasticity. Lajczok[5] used a finite difference scheme to compute the first derivatives of in-plane strain data (from the MSC/NASTRAN computer code) and then used them to find the interlaminar shear stresses with the assumption that the in-plane stresses are linear functions of the thickness coordinate. Chaudhuri[6] calculated the interlaminar stresses using a triangular element. The element is based on a layerwise constant shear angle theory and thus has a piecewise linear variation of the in-place stresses along the ply thickness direction. Chaudhuri[6] integrated the equilibrium equations of elasticity with the aid of the divergence theorem that transforms the first derivatives of in-plane stresses into the sum of in-plane stresses at midpoints on each side of the triangular element. Chaudhuri

Received June 24, 1991; revision received Feb. 27, 1992; accepted for publication March 2, 1992. This paper is declared a work of the U.S. Government and is not subject to copyright protection in the United States.

*Graduate Research Assistant, Department of Aerospace and Ocean Engineering; currently Research Scientist, MCAT Institute, San Jose, CA 95127.

†Associate Professor, Department of Aerospace and Ocean Engineering. Associate Fellow AIAA.

and Seide[7] improved the previous work by introducing a semi-analytical method that enforces transverse shear stresses to vanish at the top and bottom surfaces. Engblom and Ochoa[8] obtained interlaminar shear and normal stresses using an eight-noded quadrilateral element based on a modified Kirchhoff formulation that relaxed the Kirchhoff-Love hypothesis by superimposing shear rotations on midsurface rotations. Engblom and Ochoa assumed appropriate polynomial functions describing in-plane variation of the σ_{xz} and σ_{yz} to obtain the derivatives of those stresses with respect to in-plane coordinates, which were used to calculate the interlaminar normal stress.

Reddy[4] obtained transverse shear stresses analytically using exact closed-form solutions of symmetric cross-ply laminates using a higher-order shear deformation theory. Barbero and Reddy[9] obtained the transverse shear stresses using derivatives of in-plane stresses ($\sigma_{x,x}$, $\sigma_{y,y}$, $\sigma_{xy,x}$, and $\sigma_{xy,y}$) that were calculated by differentiating the interpolation functions of a finite element approximation that was based on a generalized laminated plate theory. These authors also used constitutive equations to obtain the transverse shear stresses.

From the perspective of predicting delamination, interlaminar normal stress is just as important as the interlaminar shear stresses. The computation of interlaminar normal stress requires one more differentiation of in-plane stresses than that necessary for the calculation of interlaminar shear stresses. However, these higher-order derivatives of in-plane stresses are not directly obtainable from a finite element code.[10] Thus some numerical procedure is necessary to construct the higher-order derivatives from finite element nodal displacement data.

In this study, a postprocessor for displacement-based finite element solutions of laminated plates under transverse loads is developed to obtain the resulting interlaminar stresses. The derivation of the formulas for the interlaminar stresses are based on the three-dimensional elasticity equilibrium equations. The formulation retains the nonlinear terms, i.e., the products of in-plane stresses and out-of-plane rotations. Bonanni et al.[11] derived the interlaminar stress equations for a *symmetric* laminated plate using the global displacement approximation that used a Fourier series approximation. The use of Fourier series to obtain continuous displacement data from the discrete infinite element data was suggested by Thurston et al.[12] to improve the accuracy of the finite element solution. The process was called "recontinuization," and the continuous Fourier series expansion was used as a first approximation in Newton's method to correct the finite element solution. These authors also provided a brief review of the existing approaches to obtain continuous data from the finite element data. Because of the Gibbs phenomenon,[13] their global displacement approximation was not good enough to calculate the higher-order derivative information.[10] To overcome this problem, a weighted least-squares technique with two different kinds of orthogonal polynomials is used in this study to obtain interpolation of the finite element nodal displacement solution, thereby facilitating the accurate calculation of various higher-order derivatives. One type consists of Chebyshev polynomials and the other of orthogonal polynomials. The latter are generated based on the distribution of nodal displacements to be approximated. Note that a least-squares approach in the past has also been used by Zienkiewicz and Zhu[14] to obtain the smoothed solution. It is also noted that in a recent paper Sistla and Thurston[15] have used a "slightly different" Fourier series expansion to overcome the Gibbs phenomenon. As a result, the recontinuization approach of Thurston and co-workers no longer suffers from Gibbs phenomenon.

The approximation using Chebyshev polynomials requires that the nodal displacements must be available at certain points: the Chebyshev points. On the other hand, the orthogonal polynomial approximation can use arbitrarily distributed displacement data. It is, however, more difficult to generate the orthogonal polynomials than the Chebyshev polynomials that are readily available. Nevertheless, it may be preferable to use orthogonal polynomials because an approximation based on these polynomials can use arbitrarily distributed displacement data points, including the displacement data at the boundary edges that cannot be used in the Chebyshev polynomial-based approximation. The displacement approximations are used to calculate derivatives of displacements with respect to in-plane coordinates.

To show the validity of this formulation, several comparisons were made with the results available in the existing literature. The postprocessor is developed in a modular fashion so that it can be easily used with any displacement-based finite element program. In this study, the postprocessor is used with two finite element programs: one based on the classical laminated plate theory (CLPT)[16] and the other based on the first-order shear deformation plate theory (FSDT).[17] For the examples studied, the present results are in good agreement with the existing data.

Interlaminar Stress Equations

The derivation of the interlaminar stress equations, σ_z, τ_{xz}, and τ_{yz}, for symmetric laminated plates is given by Bonanni et al.[11] With some modifications, these equations for the interlaminar stresses can be used for unsymmetric laminated plates of uniform thickness h as shown in Fig. 1. The midplane coincides with the x-y plane. The N layers of the plate are parallel to the x-y plane and are assumed to be homogeneous and orthotropic. The layers are numbered 1 through N from the bottom ($z = -h/2$) to the top ($z = +h/2$) of the laminate. Adjacent layers are assumed to be perfectly bonded to each other. The interface between layers k and $k+1$, where $k = 1, 2, \ldots, N-1$, is identified as the $k+1$ interface and occurs at the location $z = z_{k+1}$. The thickness of the zth layer is $h_k = z_{k+1} - z_k$, and u, v, and w denote displacements in the x-, y-, and z-coordinate directions, respectively. In what follows, the layer-dependent quantities have a superscript denoting the layer number. The elasticity equations of equilibrium for a typical layer k within the laminated plate, including the influence of the in-plane stresses on the z-directional equilibrium equation, are[11]

$$\sigma^k_{x,x} + \tau^k_{xy,y} + \tau^k_{xz,z} = 0 \tag{1}$$

$$\tau^k_{xy,x} + \sigma^k_{y,y} + \tau^k_{yz,z} = 0 \tag{2}$$

$$\tau^k_{xz,x} + \tau^k_{yz,y} + \sigma^k_{z,z} + \sigma^k_x w_{,xx} + 2\tau^k_{xy} w_{,xy} + \sigma^k_y w_{,yy} = 0 \tag{3}$$

in which body forces are neglected, and the comma convention is used to denote partial differentiation. Equations (1-3)

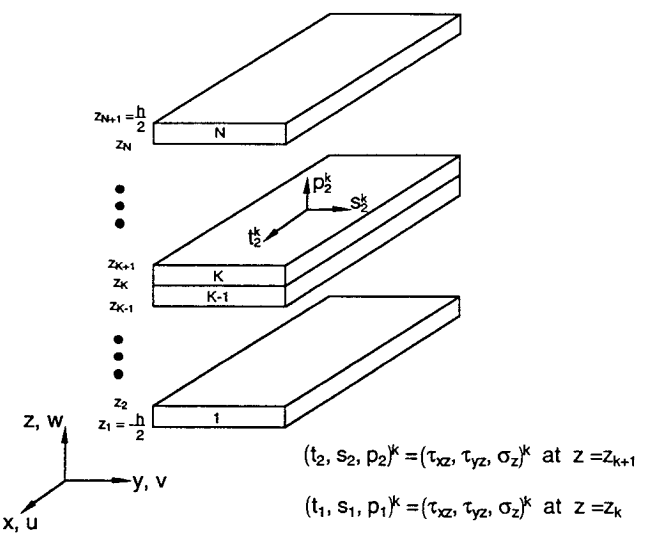

Fig. 1 Laminated plate and interlaminar stresses at $z = z_{k+1}$.

are integrated through the thickness from z_k to z_{k+1} to yield

$$N^k_{x,x} + N^k_{xy,y} + t^k_2 - t^k_1 = 0 \tag{4}$$

$$N^k_{xy,x} + N^k_{y,y} + s^k_2 - s^k_1 = 0 \tag{5}$$

$$Q^k_{x,x} + Q^k_{y,y} + N^k_x w_{,xx} + 2N^k_{xy} w_{,xy} + N^k_y w_{,yy} + p^k_2 - p^k_1 = 0 \tag{6}$$

where the lamina stress resultants are defined by

$$(N_x,\ N_y,\ N_{xy},\ Q_x,\ Q_y)^k = \int_{z_k}^{z_{k+1}} (\sigma_x,\ \sigma_y,\ \tau_{xy},\ \tau_{xz},\ \tau_{yz})^k\ dz \tag{7}$$

and the surface tractions t^k, s^k, and p^k are defined by

$$\begin{aligned} (t_2,\ s_2,\ p_2)^k &= (\tau_{xz},\ \tau_{yz},\ \sigma_z)^k \text{ at } z = z_{k+1} \\ (t_1,\ s_1,\ p_1)^k &= (\tau_{xz},\ \tau_{yz},\ \sigma_z)^k \text{ at } z = z_k \end{aligned} \tag{8}$$

The traction on the upper surface ($z = z_{k+1}$) of the kth layer is shown in Fig. 1. The out-of-plane displacement w is assumed to be independent of the thickness coordinate z, consistent with both the CLPT and the FSDT.

In Eq. (6), the shear resultants $Q^k_{x,x}$ and $Q^k_{y,y}$ can be eliminated to write the equation in terms of the stress and moment resultants. By multiplying Eq. (1) and (2) by z and then integrating them through the thickness of the layer from z_k to z_{k+1}, the two equations yield

$$M^k_{x,x} + M^k_{xy,y} + z_{k+1} t^k_2 - z_k t^k_1 - Q^k_x = 0 \tag{9}$$

$$M^k_{xy,x} + M^k_{y,y} + z_{k+1} s^k_2 - z_k s^k_1 - Q^k_y = 0 \tag{10}$$

where the lamina moment resultants are defined by

$$(M_x, M_y, M_{xy})^k = \int_{z_k}^{z_{k+1}} (\sigma_x,\ \sigma_y,\ \tau_{xy})^k\ z\ dz \tag{11}$$

Differentiating Eq. (9) with respect to x and Eq. (10) with respect to y and then substituting the resulting expressions for $Q^k_{x,x}$ and $Q^k_{y,y}$ into Eq. (6) gives the resulting equation:

$$M^k_{x,xx} + 2M^k_{xy,xy} + M^k_{y,yy} + N^k_x w_{,xx} + 2N^k_{xy} w_{,xy} + N^k_y w_{,yy} + (z_{k+1} t^k_2 - z_k t^k_1)_{,x} + (z_{k+1} s^k_2 - z_k s^k_1)_{,y} + p^k_2 - p^k_1 = 0 \tag{12}$$

Equations (4), (5), and (12) form the set of lamina equilibrium equations from which the interlaminar stress formulas are derived.

The continuity conditions of the interlaminar stresses for a perfectly bonded laminate are

$$t^k_2 = t^{k+1}_1,\ s^k_2 = s^{k+1}_1,\ p^k_2 = p^{k+1}_1, \qquad k = 1, 2, \ldots, N-1 \tag{13}$$

Using these continuity conditions and summing Eq. (4), (5), and (12) from the first to the kth layer of the laminate, one obtains the expressions for the interlaminar stresses at the $k+1$th interface in terms of the in-plane lamina stress and moment resultants and the out-of-plane displacement. These interlaminar stress equations are

$$t^k_2 = t^1_1 - \left\{ \sum_{l=1}^{k} N^l_{x,x} + \sum_{l=1}^{k} N^l_{xy,y} \right\} \tag{14}$$

$$s^k_2 = s^1_1 - \left\{ \sum_{l=1}^{k} N^l_{xy,x} + \sum_{l=1}^{k} N^l_{y,y} \right\} \tag{15}$$

$$\begin{aligned} p^k_2 = p^1_1 &- \left\{ \sum_{l=1}^{k} M^l_{x,xx} + 2\sum_{l=1}^{k} M^l_{xy,xy} + \sum_{l=1}^{k} M^l_{y,yy} \right\} \\ &- \left\{ w_{,xx} \sum_{l=1}^{k} N^l_x + 2w_{,xy} \sum_{l=1}^{k} N^l_{xy} + w_{,yy} \sum_{l=1}^{k} N^l_y \right\} \\ &- \left(z_{k+1} t^k_2 + \frac{h}{2} t^1_1 \right)_{,x} - \left(z_{k+1} s^k_2 + \frac{h}{2} s^1_1 \right)_{,y} \end{aligned} \tag{16}$$

The derivative terms $t^k_{2,x}$ and $s^k_{2,y}$ in Eq. (16) are eliminated by differentiation and substitution of Eqs. (14) and (15) into Eq. (16).

The in-plane stresses σ_x, σ_y, and σ_{xy} for the midplane can be written, if the contracted notation is used, as

$$\sigma^k_i = \sum_j \bar{Q}^k_{ij} (\epsilon^0_j + z\kappa_j) \qquad i,j = 1,2,6 \tag{17}$$

where $\bar{Q}^k_{ij}$ is the transformed reduced stiffnesses for the kth layer. Substituting this relationship into Eq. (7) for the lamina stress resultants and Eq. (11) for the lamina moment resultants yields

$$\begin{aligned} N^k_i &= \sum_j (a^k_{ij} \epsilon^0_j + b^k_{ij} \kappa_j) \\ M^k_i &= \sum_j (b^k_{ij} \epsilon^0_j + d^k_{ij} \kappa_j) \end{aligned} \qquad i,j = 1,2,6 \tag{18}$$

with

$$\begin{Bmatrix} a^k_{ij} \\ b^k_{ij} \\ d^k_{ij} \end{Bmatrix} = \begin{Bmatrix} (z_{k+1} - z_k) \\ \tfrac{1}{2}(z^2_{k+1} - z^2_k) \\ \tfrac{1}{3}(z^3_{k+1} - z^3_k) \end{Bmatrix} \bar{Q}^k_{ij} \tag{19}$$

The derivatives of the lamina stress and moment resultants can be directly obtained by differentiating Eq. (18). The interlaminar stress equations then require first and second derivatives of these midplane strains and curvatures. Using the von Kármán assumption, the relationships between strains and curvatures and displacements are written, for the CLPT, as

$$\begin{aligned} \epsilon^0_1 = \epsilon^0_x = u_{,x} + \tfrac{1}{2} w^2_{,x}, &\qquad \kappa_1 = \kappa_x = -w_{,xx} \\ \epsilon^0_2 = \epsilon^0_y = v_{,y} + \tfrac{1}{2} w^2_{,y}, &\qquad \kappa_2 = \kappa_y = -w_{,yy} \\ \epsilon^0_6 = \epsilon^0_{xy} = u_{,y} + v_{,x} + w_{,x} w_{,y}, &\qquad \kappa_6 = \kappa_{xy} = -2w_{,xy} \end{aligned} \tag{20}$$

Thus, the interlaminar stress formulas could be written in terms of displacements u, v, and w instead of midplane strains and curvatures. For the FSDT, the relations between curvatures and rotations are

$$\begin{aligned} \kappa_1 = \kappa_x &= \psi_{x,x} \\ \kappa_2 = \kappa_y &= \psi_{y,y} \\ \kappa_6 = \kappa_{xy} &= \psi_{x,y} + \psi_{y,x} \end{aligned} \tag{21}$$

where ψ_x and ψ_y are rotations of the cross sections perpendicular to the x and y axis.

Note that in this form the interlaminar shear stresses depend on second-order derivatives of the in-plane displacements and third-order derivatives of the out-of-plane displacement, whereas the interlaminar normal stress depends on third-order derivatives of the in-plane displacements and fourth-order derivatives of the out-of-plane displacement of CLPT. However, these higher-order derivatives of displacements are not directly obtainable from a finite element code. Thus some numerical procedure is necessary to construct the derivative

information from nodal displacement output obtained from a finite element program.

Furthermore, it is noted that, in the postprocessor using the FSDT, the interlaminar shear and normal stresses require second- and third-order derivatives of both displacements and rotations, respectively. Thus, as far as interlaminar stresses are concerned, the postprocessor in conjunction with the global displacement-based approximation using the FSDT may give better convergence characteristics than those obtained using the CLPT.

Displacement Approximations

The formulas for the interlaminar stresses obtained in the preceding section show that higher-order derivatives of the displacements are required than that are necessary for a weak finite element formulation. Thus, higher-order derivatives of the displacements as represented by the interpolation functions within an element cannot be expected to be very meaningful. Bonnani et al.[11] used Fourier series approximations with the discrete Fourier transform (DFT) to approximate the displacement data over the entire domain of plates. Because of the Gibbs phenomenon, the higher-order derivatives of displacements obtained using Fourier series approximation were not properly approximated.

In this study, the Chebyshev polynomials and a class of orthogonal polynomials[18] are considered to avoid the Gibbs phenomenon. As explained subsequently, the coefficients of the approximation are obtained using a least-squares technique. Let $P_r(x)$ and $P_s(y)$ be polynomials of degrees r and s in x and y, respectively, and then a global displacement distribution $w(x,y)$ may be written:

$$w(x,y) = \sum_{r=0}^{k} \sum_{s=0}^{l} C_{rs} P_r(x) P_s(y) \tag{22}$$

where C_{rs} is the undetermined coefficients for the approximation, and k and l are the approximation order of polynomials in the x and y directions, respectively. To find the approximation coefficients C_{rs}, the sum of weighted squared error between nodal displacement data and approximated displacements evaluated at the corresponding data points

$$\delta_{kl}^2 = \sum_{i=1}^{m} \sum_{j=1}^{n} a_i b_j \left[\sum_{r=0}^{k} \sum_{s=0}^{l} C_{rs} P_r(x_i) P_s(y_j) - w(x_i, y_i) \right]^2 \tag{23}$$

$$0 \le k < m \quad \text{and} \quad 0 \le l < n$$

is minimized. The m and n are the number of data points in the x and y directions, respectively, and the a_i and b_j are weighting functions corresponding to data points. By vanishing the partial derivatives of δ_{kl}^2 with respect to C_{pq}, one gets

$$\frac{\partial \delta_{kl}^2}{\partial C_{pq}} = 2 \sum_{i=1}^{m} \sum_{j=1}^{n} a_i b_j P_p(x_i) P_q(y_j) \times \left[\sum_{r=0}^{k} \sum_{s=0}^{l} C_{rs} P_r(x_i) P_s(y_j) - w(x_i, y_j) \right] = 0 \tag{24}$$

In particular, if the $P_r(x)$ and $P_s(y)$ are orthogonal over the set of all discrete displacement data with respect to the weighting function $a(x_i)$ and $b(y_j)$, that is,

$$\sum_{i=1}^{m} \sum_{j=1}^{n} A_i b_j P_r(x_i) P_s(y_j) P_p(x_i) P_q(y_j) = 0 \tag{25}$$

$$\text{for} \quad r \neq p \quad \text{or} \quad s \neq q$$

then, for $r = p$ and $s = q$, the coefficients for approximation C_{rs} are obtained as

$$C_{rs} = \frac{\sum_{i=1}^{m} \sum_{j=1}^{n} a_i b_j w(x_i, y_j) P_r(x_i) P_s(y_j)}{\sum_{i=1}^{m} \sum_{j=1}^{n} a_i b_j [P_r(x_i)]^2 [P_s(y_j)]^2} \tag{26}$$

Any function that satisfies the orthogonality condition over a set of data points (x_i, y_j) with respect to weighting functions $a(x_i)$ and $b(y_j)$ can be used to approximate global discrete displacement data by means of Eq. (26). In this study, two types of polynomials[18] that can be generated for the given location of data points are used to approximate the global displacement data.

Chebyshev Polynomials

The Chebyshev polynomials $T_r(x)$ are defined by

$$T_r(x) = \cos r\theta, \qquad x = \cos\theta \tag{27}$$

and can be readily constructed by means of a recurrence relation:

$$T_r(x) = 2xT_{r-1}(x) - T_{r-2}(x)$$
$$T_0(x) = 1 \quad \text{and} \quad T_1(x) = x \qquad r = 1,2,3, \ldots \tag{28}$$

The Chebyshev polynomial of the rth degree, $T_r(x)$, has r zeros on the interval $[-1, 1]$ and the r zeros are located at the points, called as Chebyshev abscissas,

$$x_i = \cos\left[\frac{\pi}{r}\left(i - \frac{1}{2}\right)\right], \qquad i = 1,2, \ldots, r \tag{29}$$

If displacement data are given at the points corresponding to Eq. (29), Chebyshev polynomials could satisfy the discrete orthogonality condition given by Eq. (25). Thus, the approximation using Chebyshev polynomials requires that the discrete displacement data should be available at the Chebyshev abscissas that are always in the interior region of a given domain. It is the disadvantage of the approximation using Chebyshev polynomials that the displacement data points are restricted according to Eq. (29) and the displacement data at boundary edges cannot be used in the approximation. However, the first restriction is not very strict, although, for accuracy, it will be better if the finite element nodes are provided at the Chebyshev points. In the absence of such nodes, one can easily obtain the displacement data at the Chebyshev points using the finite element displacement functions.

Orthogonal Polynomials

It will be advantageous to choose polynomials $P_r(x)$ that are orthogonal over particular discrete displacement data in the sense of Eq. (25). Then the displacement approximation using the orthogonal polynomial $P_r(x)$ has no limitation on the displacement data points. However, the $P_r(x)$ are no longer fixed polynomials but depend on each particular set of data. Forsythe[19] first obtained a satisfactory solution to generate the $P_r(x)$. In this study, a class of such orthogonal polynomials[18] is obtained and used. The $P_r(x)$ are derived by using the following recurrence formula:

$$P_{r+1}(x) = (x - \alpha_{r+1}) P_r(x) - \beta_r P_{r-1}(x)$$
$$P_0(x) = 1 \quad \text{and} \quad P_{-1}(x) = 0 \qquad r = 0,1,2, \ldots \tag{30}$$

where

$$\alpha_{r+1} = \frac{\sum_{i=1}^{m} a_i x_i [P_r(x_i)]^2}{\sum_{i=1}^{m} a_i [P_r(x_i)]^2}$$

$$\beta_r = \frac{\sum_{i=1}^{m} a_i [P_r(x_i)]^2}{\sum_{i=1}^{m} a_i [P_{r-1}(x_i)]^2}$$

and m is the number of data points. Note that the α and the β needed at each step can be computed from the two previous polynomials. Similarly, the polynomials in the y coordinate

can be constructed. Note that, for the approximation using orthogonal polynomials, the original, unnormalized x_i and y_j data points can be used, but with a considerable loss of accuracy.[20]

Numerical Results and Discussion

Although the formulation for interlaminar stress equations derived here is valid for both linear and geometrically nonlinear problems, the results in this study are obtained for linear problems only so that the present results can be compared with those available in the literature. Both the CLPT and the FSDT are used with the postprocessor developed.

The following material properties for a typical graphite/epoxy laminate are used:

$$E_1 = 1.72369 \times 10^{11}\ \text{N/m}^2, \quad E_2 = 6.894757 \times 10^9\ \text{N/m}^2$$

$$G_{12} = 3.447378 \times 10^9\ \text{N/m}^2$$

$$G_{13} = G_{23} = 1.378951 \times 10^9\ \text{N/m}^2$$

$$\nu_{12} = \nu_{13} = 0.25$$

Both symmetric and unsymmetrical laminates are considered, and simply supported boundary conditions are enforced along all of the edges. Unless stated otherwise, all of the quantities obtained are normalized as

$$(\bar{\sigma}_x, \bar{\sigma}_y, \bar{\tau}_{xy}) = \frac{1}{q_0 S^2}(\sigma_x, \sigma_y, \tau_{xy})$$

$$(\bar{\sigma}_z, \bar{\tau}_{xz}, \bar{\tau}_{yz}) = \frac{1}{q_0 S}(\sigma_z, \tau_{xz}, \tau_{yz})$$

$$S = a/h, \qquad \bar{z} = z/h$$

Cylindrical Bending Problem

For evaluative purposes, the cylindrical bending of a unidirectional orthotropic laminate subjected to sinusoidal loading along the x axis is first studied. Both ends ($x = 0$ and a) are simply supported. The geometric configuration and the loading condition are given in Fig. 2. The side-to-thickness ratio is chosen as 10.

The present solutions from the global displacement approximation using Chebyshev polynomials are compared with the exact solutions based on CLPT. Figures 3 and 4 show through-the-thickness distributions of transverse shear and normal stresses at the edge and the midpoint, respectively. When the global displacement approximation is performed using nine-point displacement data of the finite element solution at the Chebyshev abscissas, the transverse shear and normal stresses are in excellent agreement with the analytical CLPT solutions. When the global displacement approximation uses seven displacement data points, the maximum transverse shear stress obtained is 3% less than the analytical solution. However, the transverse normal stress is still in excellent agreement.

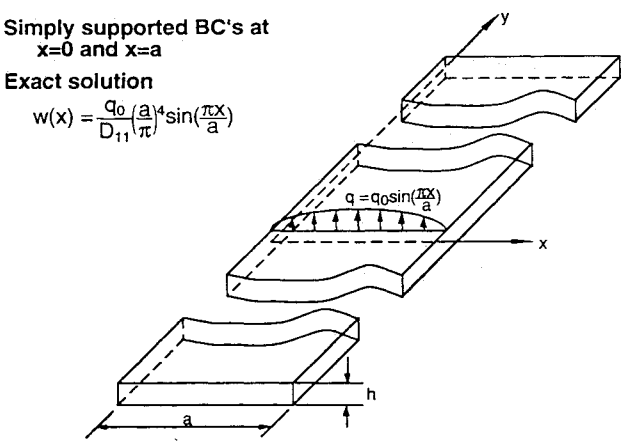

Fig. 2 Cylindrical bending of a laminated plate subjected to sinusoidal loads.

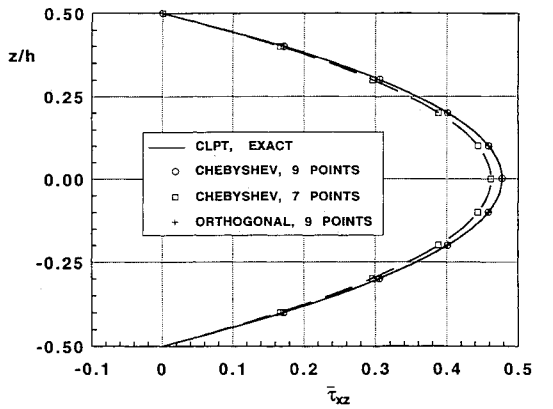

Fig. 3 Through-the-thickness distribution of transverse shear stress at the edge for cylindrical bending of a unidirectional laminate.

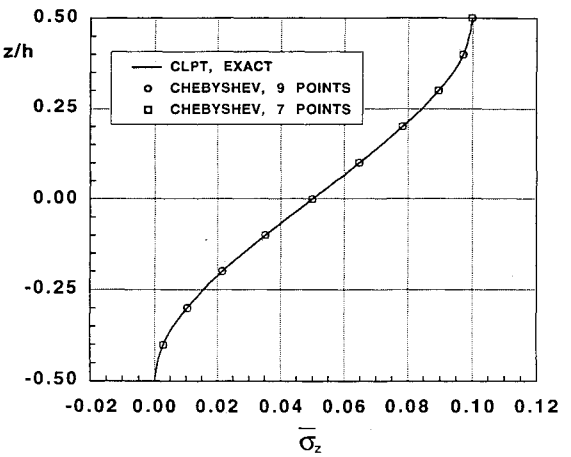

Fig. 4 Through-the-thickness distribution of transverse normal stress in the middle for cylindrical bending of a unidirectional laminate.

The result obtained using orthogonal polynomials is also compared with the aforementioned results from the Chebyshev polynomial-based approximation in Fig. 3. From the coarser mesh used in the Chebyshev polynomial-based approximation, the result obtained using the orthogonal polynomial-based approximation is in excellent agreement with the analytical CLPT solution. It is expected that the orthogonal polynomial-based approximation would give better results than the Chebyshev polynomial-based approximation since the orthogonal polynomial-based approximation could use the displacement data at the boundary edges.

The next example is the cylindrical bending of an unsymmetric laminate [0 deg/90 deg] with laminas of equal thickness subjected to a sinusoidal load along the x axis. The laminate is simply supported at both edges, and the side-to-thickness ratio is set to be 4. Through-the-thickness distributions of transverse shear and normal stresses are given in Figs. 5 and 6, respectively. The present results from the global displacement approximation using the orthogonal polynomials are compared with the elasticity solution obtained by Pagano.[1] The present results are obtained by using both the CLPT and the FSDT. The present results using the CLPT are in excellent agreement with the analytical CLPT result from Pagano.[1] For

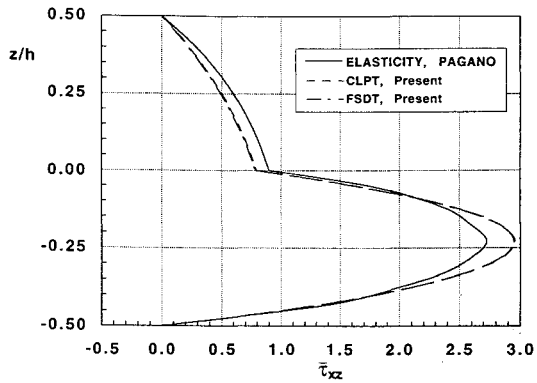

Fig. 5 Through-the-thickness distribution of transverse shear stress at the edge for cylindrical bending of a [0 deg/90 deg] laminate ($a/h = 4$, $\bar{\tau}_{xz} = \tau_{xz}(0,z)/q_0$).

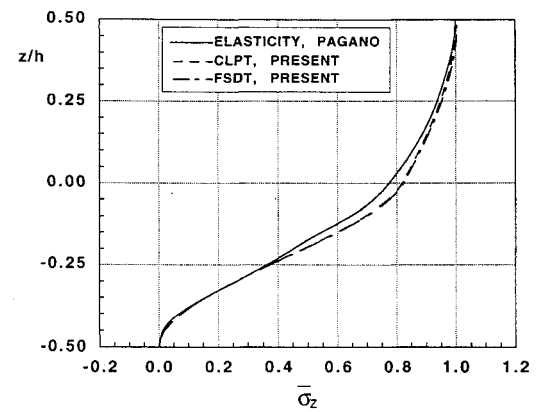

Fig. 6 Through-the-thickness distribution of transverse normal stress at the edge for cylindrical bending of a [0 deg/90 deg] laminate ($a/h = 4$, $\bar{\sigma}_z = \sigma_z(a/2,z)/q_0$).

simplicity, the analytical CLPT solution is not drawn here. The present results using the FSDT are close to the CLPT results even for the small side-to-thickness ratio in this case. The discrepancy between the elasticity solution and the present results is caused by the behavior of the in-plane displacement. Although the elasticity solution obtained by Pagano[1] shows that the in-plane displacements vary nonlinearly through the thicknesses, both CLPT and FSDT assume that the in-plane displacements vary linearly through the thickness.

Bending of Symmetrically Laminated Plates

The interlaminar stress distributions for a rectangular bidirectional symmetric laminate subjected to a doubly symmetric sinusoidal load are next obtained and compared with the existing linear elasticity solutions. The maximum amplitude q_0 of the applied load is located at the center. Simply supported boundary conditions are enforced along all four edges. The material properties used are the same as those used in the cylindrical bending problem.

Three-layered [0 deg/90 deg/0 deg] square and rectangular plates are considered for comparison. Pagano[2] has obtained the maximum stresses analytically for the same plate using both the linear elasticity theory and the classical lamination plate theory. The present results obtained using both the Chebyshev polynomial and the orthogonal polynomial approximations are compared with analytical solutions[2] in Table 1. Both the CLPT and the FSDT are used to obtain the present results. The finite element meshes are the 10×10 mesh of the full-plate model for the CLPT program and the 7×7 mesh of the quarter-plate model for the FSDT program. Both analytical and present solutions using the CLPT are in excellent agreement. The present FSDT results show that all stresses except the in-plane normal stress σ_x vary according to the trends in the elasticity solutions as the side-to-thickness ratio is changed. It is noted that the in-plane normal stress σ_x is increased in the FSDT results and decreased in the elasticity solutions as the side-to-thickness ratio is increased. Both results are converged into the CLPT solution as the side-to-thickness ratio becomes large enough. This is also observed from the finite element solution given by Reddy and Chao.[21]

Figures 7 and 8 show through-the-thickness distributions of the two transverse shear stresses $\bar{\tau}_{xz}$ and $\bar{\tau}_{yz}$ of the three-layered square laminate under a sinusoidal load. For $a/h = 10$, the maximum $\bar{\tau}_{xz}$ from the present FSDT solution is obtained to be about 6% higher than the elasticity solution,[2] and the maximum $\bar{\tau}_{yz}$ from the FSDT solution is calculated to be about 10% lower than the elasticity solution. For simplicity the elasticity solution is not drawn here. The present FSDT results show favorable prediction of transverse stresses of the symmetric laminate as compared with the elasticity solutions.

For the rectangular plate ($b/a = 3$) under a sinusoidal load, the maximum stresses are given in Table 2. Although some stress components from the elasticity solutions are not symmetric about midplane for low side-to-thickness ratios, the present solutions do not show such a behavior. An excellent agreement is shown between the analytical and present CLPT solutions.

The maximum stresses in multiple layered laminates [0 deg/90 deg/. . . /0 deg] are considered next. The total thickness for

Table 1 Maximum stresses in a three-layered square plate subjected to a sinusoidal load ($a/b = 1$)

a/h	$\bar{\sigma}_x(a/2, b/2, \pm z)$	$\bar{\sigma}_y(a/2, b/2, \pm 1/6)$	$\bar{\tau}_{xz}(0, b/2, 0)$	$\bar{\tau}_{yz}(a/2, 0, 0)$	$\bar{\tau}_{xy}(0, 0, \pm z)$
Elasticity solutions, Pagano					
10	±0.590	−0.288	0.357	0.1228	∓0.0289
20	±0.552	±0.210	0.385	0.0938	∓0.0234
100	±0.539	±0.181	0.395	0.0828	∓0.0213
Analytical CLPT solutions, Pagano					
—	±0.539	±0.180	0.395	0.0823	∓0.0213
Present results (FSDT)[a]					
10	±0.513	±0.254	0.380	0.1106	∓0.0252
20	±0.532	±0.200	0.390	0.0899	∓0.0223
100	±0.539	±0.181	0.394	0.0825	∓0.0213
Present results (CLPT)[b]					
—	±0.539[c]	±0.180	0.396	0.0824	∓0.0213
—	±0.539[d]	±0.180	0.395	0.0823	∓0.0213

[a]Quadratic isoparametric nine-node elements, 7×7 mesh, quarter-plate model, orthogonal polynomial approximation.
[b]48 degree-of-freedom thin rectangular plate elements, 10×10 mesh, full-plate model.
[c]Chebyshev polynomial approximation.
[d]Orthogonal polynomial approximation.

Table 2 Maximum stresses in a three-layered rectangular plate subjected to a sinusoidal load ($b = 3a$)

a/h	$\bar{\sigma}_x(a/2, b/2, \pm 1/2)$	$\bar{\sigma}_y(a/2, b/2, \pm 1/6)$	$\bar{\tau}_{xz}(0, b/2, 0)$	$\bar{\tau}_{yx}(a/2, 0, 0)$	$\bar{\tau}_{xy}(0, 0, \pm 1/2)$
Elasticity solutions, Pagano					
	± 0.726	$+0.0418$			-0.0120
10	-0.725	-0.0435	$0.420(\pm 0.03)$	0.0152	$+0.0123$
		$+0.0294$			
20	± 0.650	-0.0299	0.434	0.0119	∓ 0.0093
100	± 0.624	± 0.0253	0.439	0.0108	∓ 0.0083
Analytical CLPT solutions, Pagano					
—	± 0.623	± 0.0252	0.440	0.0108	∓ 0.0083
Present results (FSDT)[a]					
10	± 0.622	± 0.0375	0.438	0.0139	∓ 0.0105
20	± 0.623	± 0.0283	0.439	0.0116	∓ 0.0089
100	± 0.624	± 0.0202	0.439	0.0107	∓ 0.0083
Present results (CLPT)[b]					
—	± 0.623	± 0.0251	0.440	0.0108	∓ 0.0083

[a]Quadratic isoparametric nine-node elements, 7×7 mesh, quarter-plate model, orthogonal polynomial approximation.
[b]48 degree-of-freedom thin rectangular plate elements, 10×10 mesh, full-plate model, orthogonal polynomial approximation.

Table 3 Maximum stresses in a nine-layered square plate subjected to a sinusoidal load ($b = a$)

a/h	$\bar{\sigma}_x(a/2, b/2, \pm 1/2)$	$\bar{\sigma}_y(a/2, b/2, \pm 2/5)$	$\bar{\tau}_{xz}(0, b/2, 0)$	$\bar{\tau}_{yz}(a/2, 0, 0)$	$\bar{\tau}_{xy}(0, 0, \pm 1/2)$
Elasticity solutions, Pagano and Hatfield					
10	0.551	0.477	0.247	0.226	-0.0233
20	0.541	0.444	0.255	0.221	-0.0218
100	0.539	0.431	0.259	0.219	-0.0213
Analytical CLPT solutions, Pagano and Hatfield					
—	0.539	0.431	0.259	0.219	-0.0213
Present results (FSDT)[a]					
10	0.515	0.460	0.248	0.231	-0.0215
20	0.531	0.440	0.255	0.222	-0.0214
100	0.538	0.431	0.258	0.218	-0.0213
Present results (CLPT)[b]					
—	0.539	0.431	0.259	0.219	-0.0213

[a]Quadratic isoparametric nine-node elements, 7×7 mesh, quarter-plate model, orthogonal polynomial approximation.
[b]48 degree-of-freedom thin rectangular plate elements, 10×10 mesh, full-plate model.

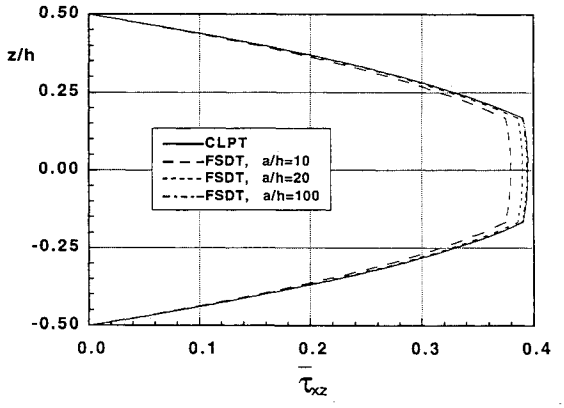

Fig. 7 Through-the-thickness distribution of $\bar{\tau}_{xz}$ of a [0 deg/90 deg/0 deg] square laminate at $x = 0$, $y = a/2$ under a doubly symmetric sinusoidal load.

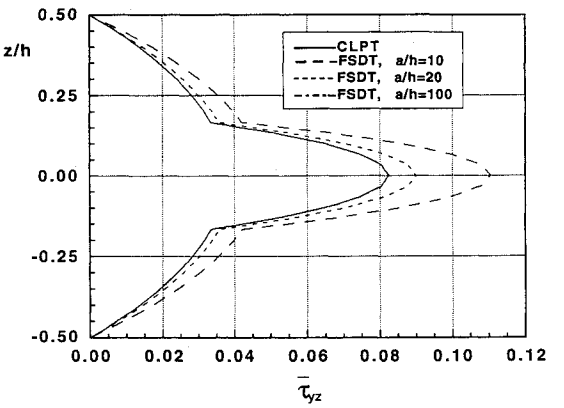

Fig. 8 Through-the-thickness distribution of $\bar{\tau}_{yz}$ of a [0 deg/90 deg/0 deg] square laminate at $x = a/2$, $y = 0$ under a doubly symmetric sinusoidal load.

the 0 and 90 deg layers are kept equal to each other with increasing number of stacking layers. The analytical elasticity and CLPT solutions of this problem are obtained by Pagano and Hatfield.[3] Using the postprocessor with both the CLPT and the FSDT, the maximum stresses for three-, five-, seven-, and nine-layered square laminates are obtained. Only the results for the nine-layered square laminate are given in Table 3. It is noted that the discrepancies between the elasticity and present FSDT solutions are reduced for large number of layers.

Bending of Unsymmetrically Laminated Plates

The final example is that of a two-layered angle-ply square laminate [− 45 deg/ + 45 deg] of length 25.4 cm and thickness

0.508 cm subjected to transverse uniform pressure q_0 ($= 6.894757 \times 10^{11}$ N/m^2) on the top surface. The -45 deg layer is the bottom layer. The material properties are the same as those of previous examples except for $E_1 = 2.757903 \times 10^{11}$ N/m^2. The plate is simply supported along all four edges such that the in-plane displacements normal to the edge are fixed, but displacements tangential to the edge are free.

For this example, Chaudhuri and Seide[7] presented the interlaminar shear stress distribution through the thickness of the laminate at a point ($x = 35a/36$, $y = 19a/36$). They obtained interlaminar shear stresses using an approximate semianalytic method, which integrates equilibrium equations of elasticity and enforces zero interlaminar shear stress condition at the bottom and top surfaces, with assumptions of transverse inextensibility and layerwise constant shear angle theory (LCST). The present result (denoted as CLPT^{BC1}) obtained at the same point is compared with that given by Chaudhuri and Seide in Fig. 9. A uniform 15×15 mesh of the full laminate for 48-degree-of-freedom elements based on the CLPT and a uniform 8×8 mesh for a quadratic isoparametric nine-node element based on the FSDT are used to obtain finite element displacement data. The orthogonal polynomials are used to approximate the global displacement data.

The present result (denoted as CLPT^{BC1}) is in excellent agreement with the analytical CLPT solution that is taken from a figure given by Chaudhuri and Seide.[7] The result (denoted as CLPT^{BC2}) from a different set of in-plane boundary conditions, namely, all in-plane displacements are fixed along the edges, is also obtained. It is seen that, because of the existence of nonzero in-plane displacements, the maximum interlaminar stress $\bar{\tau}_{xz}$ is approximately increased by 20% as changing the boundary condition from the CLPT^{BC1}

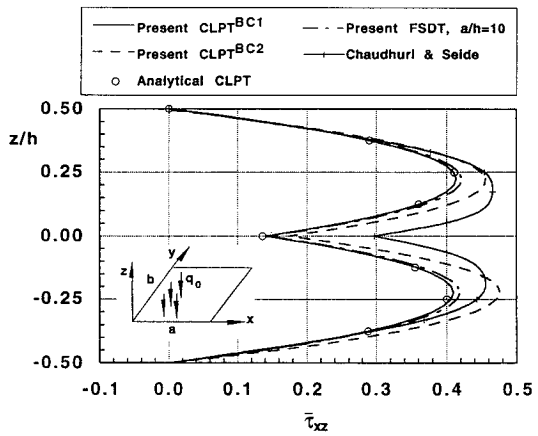

Fig. 9 Through-the-thickness distribution of $\bar{\tau}_{xz}$ of the unsymmetric angle-ply at $x = 35a/36$, $y = 19a/36$.

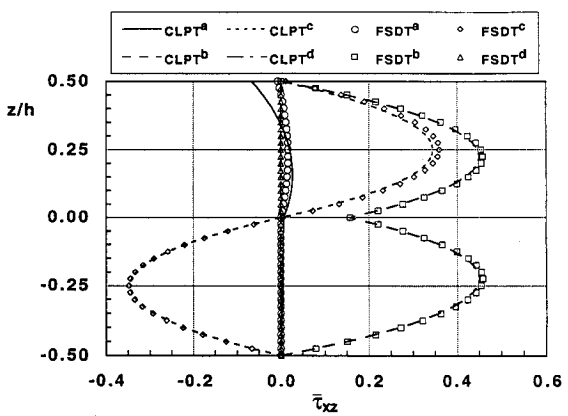

Fig. 10 Through-the-thickness distribution of $\bar{\tau}_{xz}$ at four different points of the unsymmetric angle-ply laminate.

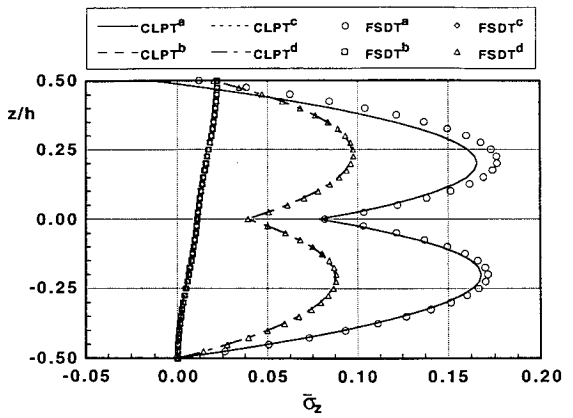

Fig. 11 Through-the-thickness distribution of $\bar{\sigma}_z$ at four different points of the unsymmetric angle-ply laminate with $a/h = 50$.

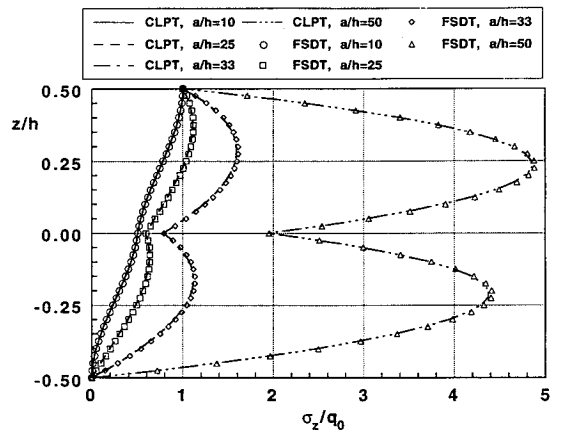

Fig. 12 Variation of through-the-thickness distribution of interlaminar normal stress at the center with varying side-to-thickness ratio of unsymmetric angle-ply laminates.

case to the CLPT^{BC2} case. Using the same boundary condition as that used in the CLPT^{BC1} case, the present FSDT result is obtained for $a/h = 10$. The FSDT result predicted a little higher value than the CLPT result. The results from Chaudhuri and Seide[7] predicted higher values than the present results. Since, for a thick plate, in-plane displacements do not vary linearly through the thickness, it is expected that the result based on the LCST will be different from the present results (as was the case in the cylindrical bending problem).

To see the convergence characteristics of interlaminar shear and normal stresses at the top surface, four typical points (one corner point, two midpoints of edges in the x and y directions, and the center point) are selected. In Fig. 10, through-the-thickness distribution of interlaminar shear stress $\bar{\tau}_{xz}$ at the four points is presented using both the CLPT and FSDT. The superscripts a, b, c, and d denote the four points ($x = 0$, $y = 0$), (0, $b/2$), ($a/2$, 0), and ($a/2$, $b/2$), respectively. The interlaminar shear stress condition at the surface is well satisfied except at the corner point. Although Chaudhuri and Seide[7] stated that the integration of equilibrium equations of elasticity, as applied to an unsymmetric angle-ply plate, may not yield accurate results, the present method, which integrates equilibrium equations, could obtain accurate results except at the corner point. It suggests that the approximation of global displacements may be very accurate so as to minimize the error in calculation of higher-order derivatives used in the integration of elasticity equilibrium equations. The difference between the FSDT results for $a/h = 10$ and the present CLPT results is small in this case. It is noted that, at the corner point, the FSDT result converged better than the CLPT result. This is because, in the postprocessor using the FSDT, only

third-order derivatives of both displacements and rotations are required to calculate the interlaminar normal stress, whereas in the postprocessor using the CLPT, fourth-order derivatives of the out-of-plane displacement are needed. Similar behavior was observed for $\bar{\tau}_{yz}$.

In Fig. 11, through-the-thickness distribution of interlaminar normal stress of the unsymmetric angle-ply laminate at the four points is shown. The side-to-thickness ratio of the unsymmetric angle-ply laminate used is 50. For the prediction of delamination, interlaminar normal stress is as important as the interlaminar shear stresses. However, to the best of our knowledge, this is the first paper where the interlaminar normal stress for an unsymmetric angle-ply laminate has been obtained from the CLPT and the FSDT displacement data. The present method could calculate the interlaminar normal stress accurately except at the corner point. It should be noted that the maximum interlaminar normal stresses at the center and the corner point are approximately 4.5 and 8 times higher than the applied pressure, respectively. From Figs. 10 and 11, it is noted that the interlaminar normal stress is dominant at the corner and the center and the interlaminar shear stresses at the midpoints of the edges.

The variation of through-the-thickness distribution of interlaminar normal stress at the center with varying side-to-thickness ratio of unsymmetric angle-ply laminates is presented in Fig. 12. In this figure, the interlaminar normal stress is normalized using the applied load only to see the changes of the magnitude of the interlaminar normal stress according to various side-to-thickness ratios. The results are obtained for four side-to-thickness ratios: 10, 25, 33, and 50. It is seen that the differences between the results from both the CLPT and the FSDT are very small in this problem. However, there are significant changes of through-the-thickness distribution of σ_z as the side-to-thickness ratio changes. In this problem, the maximum normal stress is 4.8 times higher than the applied pressure at the center of the unsymmetric angle-ply laminate for $a/h = 50$. It is observed that the maximum interlaminar stress increases rapidly as the side-to-thickness ratio increases.

Concluding Remarks

In this paper, a postprocessor that can calculate interlaminar shear and normal stresses of laminated plates subjected to transverse loads is developed. The postprocessor is in a modular form and can be easily adapted to any displacement-based finite element program. The postprocessor can be used for both the classical laminated plate theory and the first-order shear deformation theory. It uses the global displacement approximation to calculate the derivative information of in-plane stresses. Two types of polynomials, Chebyshev and a class of orthogonal polynomials,[18] are used in the global displacement approximation. The present global displacement approximation can give very accurate higher-order derivatives of displacements.

The interlaminar stresses are presented for cylindrical and plate bending problems with all of the edges having simply supported boundary conditions. The laminates are subjected to the sinusoidally distributed symmetric loads. Whenever possible, present results are compared with the results available in the existing literature. A good agreement is obtained. For an example nine-layered square laminated plate considered in this study, it is seen that the interlaminar stresses obtained using the FSDT are in good agreement with those obtained from the analytical elasticity solution.

The present method could calculate the interlaminar normal and shear stresses for an unsymmetric angle-ply laminate subject to uniformly distributed pressure loads accurately except at points near the corner. To the best of our knowledge, this paper is first to obtain interlaminar normal stress in an unsymmetric angle-ply laminate by only using the nodal displacement data. It is observed that the maximum interlaminar normal stresses of the unsymmetric angle-ply laminate with $a/h = 50$ are four to eight times higher than the applied pressure load. It should be noted that the shape of through-the-thickness distribution of interlaminar normal stress depends on the side-to-thickness ratio, and the maximum interlaminar normal stress increases rapidly as the side-to-thickness ratio increases.

This postprocessor can be used to improve the accuracy of the finite element solutions (deformations and vibration frequencies) based on the CLPT and the FSDT in conjunction with a two-phase computational procedure as suggested by Noor and Burton.[22] The two-phase computational procedure corrects the global responses (vibration frequencies and deformations) obtained from a two-dimensional first-order shear deformation theory by using the equilibrium equations and constitutive relations of the three-dimensional theory of elasticity.

At present, interlaminar stresses of laminates that have different boundary conditions and are subjected to distributed moment loads are being studied. The effect of geometric nonlinearities on the interlaminar stresses in laminated plates subjected to dynamic impact loads is also being studied.

Acknowledgments

A portion of the research described in this paper was carried out under a grant from the Army Research Office (Grant DAALO3-90-G-0134). The authors gratefully acknowledge the support of Gary L. Anderson, the projector monitor. The authors also acknowledge substantial technical help from E. R. Johnson and J. N. Reddy.

References

[1]Pagano, N. J., "Exact Solutions for Composite Laminates in Cylindrical Bending," *Journal of Composite Materials,* Vol. 3, July 1969, pp. 398–411.

[2]Pagano, N. J., "Exact Solutions for Rectangular Bidirectional Composites and Sandwich Plates," *Journal of Composite Materials*, Vol. 4, 1970, pp. 20–34.

[3]Pagano, N. J., and Hatfield, S. J., "Elastic Behavior of Multilayered Bidirectional Composites," *AIAA Journal*, Vol. 10, No. 7, 1972, pp. 931–933.

[4]Reddy, J. N., "A Simple Higher-Order Theory for Laminated Composite Plates," *Journal of Applied Mechanics*, Vol. 51, Dec. 1984, pp. 745–752.

[5]Lajcok, M. R., "New Approach in the Determination of Interlaminar Shear Stresses from the Results of MSC/NASTRAN," *Computers and Structures*, Vol. 24, No. 4, 1986, pp. 651–656.

[6]Chaudhuri, R. A., "An Equilibrium Method for Prediction of Transverse Shear Stresses in a Thick Laminated Plate," *Computers and Structures*, Vol. 23, No. 2, 1986, pp. 139–146.

[7]Chaudhuri, R. A., and Seide, P., "An Approximate Semi-Analytical Method for Prediction of Interlaminar Shear Stress in an Arbitrary Laminated Thick Plate," *Computers and Structures*, Vol. 25, No. 4, 1987, pp. 627–636.

[8]Engblom, J. J., and Ochoa, O. O., "Finite Element Formulation Including Interlaminar Stress Calculations," *Computers and Structures*, Vol. 23, No. 2, 1986, pp. 241–249.

[9]Barbero, E. J., and Reddy, J. N., "On a Generalized Laminate Plate Theory with Application to Bending, Vibration and Delamination Buckling in Composite Laminates," Center for Composite Materials and Structures, CCMS-89-20, Virginia Polytechnic Inst. and State Univ., Blacksburg, VA, Oct. 1989.

[10]Johnson, E. R., and Bonanni, D. L., "Order 2*p* Derivatives from *p*-Differentiable Finite Element Solutions by a Spectral Method," *Proceedings of the 3rd International Conference on CAD/CAM Robotics and Factories of the Future*, Vol. 1, Springer-Verlag, Berlin, 1989, pp. 134–138.

[11]Bonanni, D. L., Johnson, E. R., and Starnes, J. H., Jr., "Local Buckling and Crippling of Composite Stiffener Sections," Center for Composite Materials and Structures, CCMS-88-08, Virginia Polytechnic Inst. and State Univ., Blacksburg, VA, June 1988, pp. 126–158.

[12]Thurston, G. A., Reissner, J. E., Stein, P. A., and Knight, N. F., Jr., "Error Analysis and Correction of Discrete Solutions from Finite Element Codes," *AIAA Journal*, Vol. 26, No. 4, 1988, pp. 446–453.

[13]Fletcher, C. A. J., *Computational Galerkin Methods,* Springer-Verlag, New York, 1984, pp. 189, 190.

[14]Zienkiewicz, O. C., and Zhu, T. Z., "A Simple Error Estimator and Adaptive Procedure for Practical Engineering Analysis," *Inter-*

national Journal for Numerical Methods in Engineering, Vol. 24, No. 2, 1987, pp. 337–357.

[15]Sistla, R., and Thurston, G. A., "An Improved Error Analysis of Finite Element Solutions for Postbuckled Plates," AIAA Paper 91-1003, 1991.

[16]Kapania, R. K., and Yang, T. Y., "Buckling, Postbuckling, and Nonlinear Vibrations of Imperfect Plates, *AIAA Journal*, Vol. 25, No. 10, 1987, pp. 1338–1346.

[17]Reddy, J. N., "A Penalty Plate-Bending Element for the Analysis of Laminated-Anisotropic Composite Plates," *International Journal for Numerical Methods in Engineering*, Vol. 15, 1980, pp. 1187–1206.

[18]Ralston, A., *A First Course in Numerical Analysis*, 1st ed., McGraw-Hill, New York, 1965, pp. 228–270.

[19]Forsythe, G. E., "Generation and Use of Orthogonal Polynomials for Data Fitting with a Digital Computer," *Journal of Society of Industrial and Applied Mathematics*, Vol. 5, No. 2, 1957, pp. 74–82.

[20]Hayes, J. G., "Curve Fitting by Polynomials in One Variable," *Numerical Approximation to Functions and Data*, 1st ed., Athlone Press, London, 1970, pp. 43–64.

[21]Reddy, J. N., and Chao, W. C., "A Comparison of Closed-Form and Finite-Element Solutions of Thick Laminated Anisotropic Rectangular Plates," *Nuclear Engineering and Design*, Vol. 64, 1981, pp. 153–167.

[22]Noor, A. K., and Burton, W. S., "Stress and Free Vibration Analysis of Multilayered Composite Plates," *Composite Structures*, Vol. 11, 1989, pp. 183–204.

Recommended Reading from
Progress in Astronautics and Aeronautics

MECHANICS AND CONTROL OF LARGE FLEXIBLE STRUCTURES

J.L. Junkins, editor

This timely tutorial is the culmination of extensive parallel research and a year of collaborative effort by three dozen excellent researchers. It serves as an important departure point for near-term applications as well as further research. The text contains 25 chapters in three parts: Structural Modeling, Indentification, and Dynamic Analysis; Control, Stability Analysis, and Optimization; and Controls/Structure Interactions: Analysis and Experiments. *1990, 705 pp, illus, Hardback, ISBN 0-930403-73-8, AIAA Members $69.95, Nonmembers $99.95, Order #: V-129 (830)*

Place your order today! Call 1-800/682-AIAA

AIAA

American Institute of Aeronautics and Astronautics
Publications Customer Service, 9 Jay Gould Ct., P.O. Box 753, Waldorf, MD 20604
Phone 301/645-5643, Dept. 415, FAX 301/843-0159

Sales Tax: CA residents, 8.25%; DC, 6%. For shipping and handling add $4.75 for 1-4 books (call for rates for higher quantities). Orders under $50.00 must be prepaid. Please allow 4 weeks for delivery. Prices are subject to change without notice. Returns will be accepted within 15 days.